[CANCER RESEARCH 64, 3444–3451, May 15, 2004]

Telomeric Recombination in Mismatch Repair Deficient Human Colon Cancer Cells after Telomerase Inhibition

Oliver E. Bechter,[1] Ying Zou,[2] William Walker,[2] Woodring E. Wright,[2] and Jerry W. Shay[2]

[1]University of Innsbruck, Department of Internal Medicine, Innsbruck, Austria and [2]University of Texas Southwestern Medical Center, Department of Cell Biology, Dallas, Texas

ABSTRACT

The majority of human malignancies use telomerase to maintain telomere homeostasis. Antitelomerase therapy is therefore a promising approach for a cancer-specific therapy. The alternative lengthening of telomeres pathway (ALT) is a recombination-based, telomerase-independent mechanism of telomere length control. It is widely believed that ALT could be engaged when cancer cells escape from telomerase inhibition. However, no reports exist that would support this concept of therapy resistance. We inhibited telomerase in a human cancer cell line with a mismatch repair defect and observed a telomerase-independent, ALT-like telomere elongation. This is the first report of inducing a telomerase-independent telomere elongation in human cancer cells when telomerase is inhibited, thus describing a novel mechanism of resistance to antitelomerase therapy.

INTRODUCTION

Cellular immortality requires a mechanism that replenishes telomeric DNA. In all cells, telomeres shorten with each round of cell division caused in part by incomplete lagging strand synthesis as well as to poorly defined end processing nucleases (1–3). If compensatory mechanisms are lacking, this process leads to replicative senescence in normal cells when short telomeres trigger a p53-regulated DNA damage response (4). In the presence of cancer mutations such as p53, which can bypass the initial senescence checkpoint arrest, increased genomic instability, chromosomal end fusions, and cell death occurs as a result of critically short telomeres leading to cycles of breakage-fusion and eventual mitotic catastrophe (5).

Two mechanisms existing *in vivo* as well as *in vitro* have been identified to maintain telomere homeostasis in cells with infinite-replicative potential. Telomerase, a ribonucleoprotein reverse transcriptase that adds repetitive DNA sequences to telomeric ends, is the preferred pathway for cell immortalization (6). The fact that >90% of human cancer cells *in vivo* show the presence of telomerase activity suggests the importance of this mechanism for tumor cells to divide without limits (7). The second mechanism for maintaining telomere length is commonly known as the alternative lengthening of telomeres pathway (ALT; Ref. 8). Currently ALT is defined by the lack of detectable telomerase activity plus the capacity of limitless divisions. ALT cells usually exhibit a remarkable heterogeneous telomere length in a given cell, often ranging from >20 kb to <2 kb. ALT cells also contain ALT-associated promyelocytic leukemia bodies (APBs) in about 5% of interphase nuclei. APBs in ALT cells have been shown to contain telomeric DNA, telomere-binding proteins, as well as proteins involved in DNA recombination and replication in conjunction with promyelocytic leukemia protein. There is mounting evidence that the mechanism by which ALT cells maintain their telomeres is based on homologous recombination (9). Because ALT cells do not have a general defect in the recombination machinery (10), there may be a telomere-specific recombination defect that allows ALT cells to recombine critically short telomeres to maintain sustained cellular proliferation.

Antitelomerase therapy is a promising approach, which more specifically affects cancer cells (11). There are many different ways to disrupt enzyme activity or its physiological function. Therefore, one can expect to achieve efficient telomere dysfunction especially if different approaches are combined. Although theoretical, there is concern about the possibility of therapy resistance occurring if cancer cells were to engage the ALT pathway after telomerase inhibition. In the present study, we tested whether a pre-existing mismatch repair (MMR) defect in a colon cancer cell line might facilitate engagement of ALT after the inhibition of telomerase. Mismatch repair proteins inhibit homologous recombination between imperfectly matched sequences (12), whereas MMR defects increase homologous recombination between diverged sequences (13). Loss of MMR function in yeast increases the viability of cells lacking telomerase (14). Thus the focus of the present study was to determine whether MMR insufficiency would facilitate engagement of the ALT pathway to heal critically short telomeres in the absence of telomerase.

Our data show, for the first time, that telomere elongation without the reappearance of telomerase activity can occur in a cancer cell line with a MMR defect when telomerase is inhibited. This ALT-like elongation event is associated with the presence of an ongoing homologous recombination process between sister chromatids [telomeric sister chromatid exchange (T-SCE)], and we now report that T-SCE is a characteristic of all established ALT cells analyzed. Furthermore, cancer cells responding with T-SCE after telomerase inhibition are less tumorigenic in a nude mouse model, which has been shown to be an additional characteristic of ALT cells (15). In summary, we describe a mechanism of resistance to antitelomerase therapy in the presence of a MMR defect.

MATERIALS AND METHODS

Cell Culture and Viral Infection. All cells were grown at 37°C in a 4:1 mixture of Dulbecco's modified Eagle's medium and Medium 199 (Invitrogen, Carlsbad, CA) including 10% cosmic calf serum (Hy Clone Laboratories, Logan, UT). HCT 15 [human MutS homologue 6 (hMSH6) -/-], HCT 116 (human mutL homolog 1 -/-), Lovo (hMSH2 -/-) and SW480 (wild type) colon cancer cells were obtained from the American Type Culture Collection cell repository. Generation of retroviral particles was accomplished by transfecting (Fugene; Roche, Indianapolis, IN) 30 μg of plasmid DNA encoding for the dominant-negative human telomerase reverse transcriptase (hTERT) linked to the *blasticidin* resistance gene via an internal ribosomal entry site sequence (pWZL Blast D869A) into PhoenixE packaging cells. After 48 h, supernatant was harvested and used for infecting the amphotropic packaging cell PA317 as described previously (16). Supernatant of blasticidin-selected PA317 cells was then used to infect target cells. After selection with 30 μg/ml blasticidin (Invitrogen), individual clones were picked and kept under selection throughout the experiment. Fluctuation analysis to determine the frequency of cells escaping from crisis events was done as described previously (17).

Full-length MSH6 cDNA was kindly provided by J. Jiricny (18). A 4.2 kb fragment was isolated with *Bam*H I and *Xho*I from pBluescript hMSH6 and

Received 1/31/04; revised 3/30/04; accepted 4/2/04.

Grant support: This work was supported by the National Institute on Aging, AG07992, fellowships to O. E. Bechter from the "Erwin Schroedinger Auslandsstipendium" (J2214) of the FWF, Austrian Science Fund, the Department of Defense Breast Cancer Research Program, DAMD 17-03-1-0468, and the Ellison Medical Foundation.

The costs of publication of this article were defrayed in part by the payment of page charges. This article must therefore be hereby marked *advertisement* in accordance with 18 U.S.C. Section 1734 solely to indicate this fact.

Requests for reprints: Jerry W. Shay, University of Texas, Southwestern Medical Center, Department of Cell Biology, 5323 Harry Hines Blvd., Dallas, Texas 75390-9039. Phone: (214) 648-3282; Fax: (214) 648-8694; E-mail: jerry.shay@utsouthwestern.edu.

cloned into pWZL-Blast using the same restriction sites. pWZL-Blast hMSH6 was digested with *Bam*H I and *Sal*I and ligated into the pBabe-Puro retroviral vector using the corresponding restriction sites. Expression of MSH6 protein was verified by transient transfection of 10-μg plasmid DNA into HCT 15 cells and subsequent Western blotting.

Adenoviral hTERT infection (kindly provided by Geron Corp.) was done at 30 multiplicity of infections every 4 days on cells at 2nd crisis. Restoration of telomerase activity as well as telomere length and T-SCE was monitored as described below.

Telomere Restriction Fragment (TRF) and Telomere Repeat Amplification Protocol (TRAP) Analysis. For measuring telomere length, 2×10^6 cells were collected and resuspended in 60 μl of 100 mM NaCl, 100 mM EDTA (pH 8.0) and 10 mM Tris (pH 8.0). Triton X 100 and Proteinase K (Roche) were added to a final concentration of 1% and 2 mg/ml, respectively. After digestion at 55°C for 12 h, proteinase K was inactivated at 70°C for 30 min. Samples were dialyzed for 16 h against a TE buffer [10 mM Tris (pH 8.0), 0.1 mM EDTA (pH 8.0)], and 1 μg of genomic DNA was subjected to digestion with 6 enzymes (*Alu*I, *Cfo* I, *Hae*I, *Hinf* I, *Msp*I, and *Rsa*I) for 6 h. Digested DNA was run on a 1% agarose gel using a Fige Mapper (Bio-Rad, Hercules, CA) alternating from 180 V forward to 180 V backward in decreasing intervals of 0.1–0.8 s at 14°C. After denaturing (0.5 M NaOH, 1.5 M NaCl) for 20 min, the gel was rinsed in H_2O for 10 min, dried at 56°C for 3 h, and finally neutralized (1.5 M NaCl, 0.5 M Tris). After neutralization, hybridization with a P^{32}-labeled $(TTAGGG)_4$ oligonucleotide was performed at 42°C for 16 h. After washing the gel once in $2 \times$ SSC [$1\times = 0.15$ M NaCl, 0.015 M Na citrate (pH 7.0)] for 15 min at room temperature followed by two washes with $0.1 \times$ SSC/0.1% SDS for 10 min at room temperature, the gel was exposed to a phosphor screen and analyzed on Storm 860 Phosphor Imager (Molecular Dynamics, NJ). The mean telomere length was calculated as described previously (19) using the program Telorun (available at http://www.swmed.edu/home_pages/cellbio/shay-wright/research/sw_lab_methods.htm).

Telomerase activity was measured using a TRAPeze kit (Intergen, Purchase, NY) following the basic protocol of the manufacturer. For each assay, the equivalent of 1000 cells was used, and PCR amplification was done for 30 cycles. At each crisis event, as well as before and after, individual samples were analyzed at least twice under different conditions. The cell number per reaction was increased up to 10,000 cells (1,000, 2,000, 5,000, and 10,000 increments) yielding the same result as shown in Fig. 2*A*. Quantitation and visualization of the TRAP gels was done as described previously (20).

Chromosomal Orientation Fluorescence *in Situ* Hybridization and Conventional Fluorescence *in Situ* Hybridization (FISH) Analysis. Chromatid orientation (CO)-FISH analysis was done following the basic protocol established by Goodwin *et al.* (21) and Bailey *et al.* (22) with several modifications. Briefly, sub-confluent cell monolayers were cultured into medium containing a 3:1 ratio of 5′-bromo-2′-deoxyuridine:5-bromodeoxycytidine (Sigma, St. Louis, MO) at a total final concentration of 1×10^{-5} M for 24 h, and Colcemid (0.2 μg/ml) was added for the final 4 h. Metaphase spreads were prepared by treating trypsinized cells with hypotonic KCl buffer (0.075 M) for 30 min at 37°C followed by several washes with methanol-acetic acid (3:1) until a clean white pellet was obtained. The pellets were stored at −20°C, then cells were spread on slides. Slides were treated with RNase A (0.5 mg/ml) for 10 min at 37°C, stained with Hoechst 33258 (0.5 μg/ml; Sigma) for 15 min at room temperature, mounted with McIlvaine's buffer (at pH 8.0), and exposed to 365-nm UV light (Stratelinker 1800 UV irradiator) for 30 min at 55°C. The bromodeoxyuridine:5-bromodeoxycytidine-substituted DNA was digested with Exonuclease III (3 units/μl; Promega, Madison, WI) in 50 mM Tris-HCl (pH 8.0), 5 mM $MgCl_2$, and 5 mM DTT for 10 min at room temperature. The C-rich strands (templates for leading strand synthesis) were revealed by hybridizing (20 μl) in 70% formamide, 20 ng of 3′-Cy3-conjugated $(TTAGGG)_3$ 2′-deoxyoligonucleotide $N_{3'}$-$P_{5'}$ phosphoramidate probe (kindly provided by Sergei Gryaznov, Geron Corp.), 0.25% (w/v) blocking reagent (Roche), and 5% $MgCl_2$ in 10 mM Tris (pH 7.2), which was added to the slides containing single-stranded chromosomal target DNA without denaturation. After 2 h incubation at room temperature, the slides were washed twice with 70% formamide, 0.1% BSA, 10 mM Tris (pH 7.2) and washed twice with 0.15 M NaCl, 0.05% Tween 20, and 0.05 M Tris. The slides were then dehydrated through an ethanol series (70, 85, and 100%), and air-dried in the dark. The G-rich strands (templates for lagging strand synthesis) were then visualized by incubating with a second hybridization mixture (20 μl) containing 70% formamide, 20 ng of 3′-FITC-conjugated $(CCCTAA)_3$ 2′-deoxyoligonucleotide $N_{3'}$-$P_{5'}$ phosphoramidate probe (kindly provided by Sergei Gryaznov, Geron Corp.), 0.25% (w/v) blocking reagent (Roche), and 5% $MgCl_2$ in 10 mM Tris, pH 7.2, for 2 h at room temperature. The slides were then washed, dehydrated and air-dried in the dark. Conventional FISH analysis was done following the protocol described previously (23). Chromosomes were counterstained with 4′,6-diamidino-2-phenylindole (0.6 μg/ml; Vector Laboratories, Burlingame, CA) for chromosome identification, and slides were digitally imaged on a Zeiss Axioplan 2 microscope (63× and 100×; 1.4 numerical aperture; Plan-Apochromat oil immersion objective) with precision Cy3/FITC/4′,6-diamidino-2-phenylindole bandpass filter sets. Cy3, FITC, and 4′,6-diamidino-2-phenylindole images were captured separately with a CCD (Hamamatsu) camera, merged using Openlab software, and further processed using Adobe Photoshop version 5.5 software.

Western Blotting and Immunofluorescence for APB Body Staining. Nuclear extracts for protein analysis were prepared as described previously (18). Total protein concentration was determined using a bicinchoninic acid assay (Pierce, Rockford, IL) according to the manufacturer's instructions. A total of 50 μg of nuclear extracts were loaded on a 7% SDS-polyacrylamide gel. After electrophoresis, the proteins were transferred onto a polyvinylidene difluoride membrane for 90 min at 120 V, 4°C following the manufacturer's protocol (Millipore, Bedford, MA). After transfer, the membrane was blocked with 5% low fat milk phosphate buffered saline + 0.05% Tween for 1 h at room temperature. The primary antibody to detect MSH6 was used at a dilution of 1:200 in blocking buffer and incubated for 16 h at 4°C (mouse monoclonal; BD Transduction Laboratories, San Diego, CA). After three washes with phosphate buffered saline + 0.05% Tween the secondary antimouse antibody conjugated with alkaline phosphatase was applied for 1 h at room temperature at a dilution of 1:9000 (Amersham, Little Chalfont, Buckinghamshire, United Kingdom). A conventional chemiluminescence system was used to visualize proteins following the manufacturer's instruction (Pierce).

For detection of APB bodies, cells were grown on cover slips at 37°C for 24 h. The staining procedure was performed as described previously (23) using mouse antipromyelocytic leukemia protein (Santa Cruz Biotechnology, Santa Cruz, CA) and rabbit antihuman TRF2 (Santa Cruz Biotechnology). Visualization was done by incubation with fluorescein-conjugated goat antimouse and rhodamine-conjugated donkey antirabbit secondary antibodies (Molecular Probes, Leiden, the Netherlands). Counterstaining was performed with 4′,6-diamidino-2-phenylindole (Vector Laboratories) and images were acquired on a Zeiss Axioplan 2 microscope.

***In Vivo* Tumor Formation.** Athymic nude mice were purchased from Harlan Sprague Dawley Inc. and kept and used in accordance with institutional guidelines. To produce tumors, 5×10^6 cells grown in log phase were washed in PBS and resuspended in 200 μl. Cells (5×10^6) were injected into each flank. There were no signs of cell death, and cells grew at the same proliferation rate at the time of injection. After sacrificing the animal, tumor volume was calculated according to the following formula: $0.5 \times (\text{length}) \times (\text{width})^2$.

RESULTS

Telomere Length Kinetics in an MSH6 −/− Clone Expressing a Dominant-Negative hTERT. HCT 15 human colon cancer cells expressing telomerase activity were infected with a retrovirus encoding a dominant-negative hTERT, and individual clones were isolated. Telomere dynamics were followed in five clones. Fig. 1*A* shows a TRF analysis of one of the clones. Twenty population doublings (PDs) after infection, median telomere length was 2.6 kb with the cells dividing at 1 PD/1.5 days. Continuous telomere shortening was observed until PD 36 when cells entered crisis (1st crisis). This crisis was associated with a decrease in the proliferation rate to 1 PD/5 days, the occurrence of vacuolated cells and a high rate of cell death (crisis). After 10 days in crisis multiple foci of rapidly dividing cells (~1 PD/day) emerged. Telomere length analysis immediately after PD 36 showed a telomere elongation from 2.6 kb to a median length of 5.1 kb with the appearance of a discrete band at ~9 kb. Cells were followed through crisis as a population. Fluctuation analysis to determine the frequency of this event showed that approximately 1 in 3000

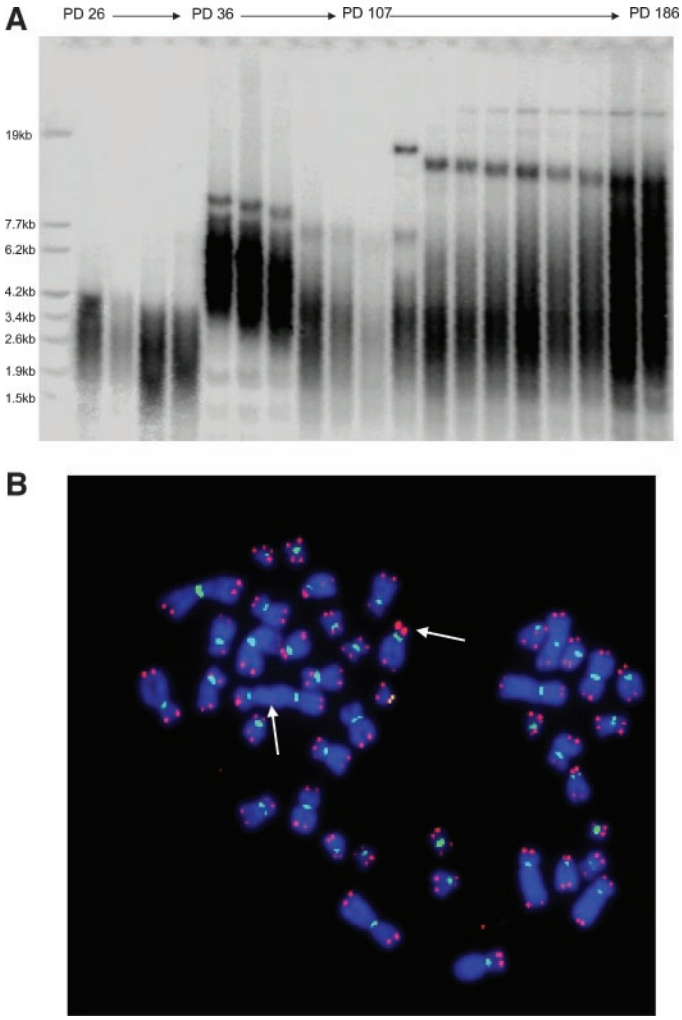

Fig. 1. *A*, telomere length kinetics in an HCT 15 clone expressing a dominant-negative human telomerase reverse transcriptase. Telomeres gradually shorten until population doubling 36, where cellular crisis (1st crisis) occurs. One in 3000 cells emerges from 1st crisis, displaying elongated telomeres that subsequently shorten. At population doubling 107, another crisis occurred (2nd crisis) with 1 in 200 cells escaping, showing another telomere elongation event and the appearance of a distinct high molecular weight band at ~16 kb. *B*, FISH analysis after the 2nd crisis event. Two crisis events and the result of critically short telomeres lead to some chromosomal end-to-end fusions (*left arrow*). The distinct high molecular weight band shown in the telomere restriction fragment analysis corresponds to the chromosome with a very intense telomeric signal (*right arrow*).

cells were able to escape 1st crisis. The cellular proliferation rate after 1st crisis was approximately 1 PD/1.5 days accompanied with ongoing telomere shortening. At PD 107, when median telomere length was ~3.0 kb, a 2nd crisis event occurred (with the same phenotype and proliferation rate decrease as during 1st crisis except for being noticeably milder). After 7 days, foci of rapidly dividing cells appeared with a frequency of 1 in 200 cells. TRF analysis after PD 107 was distinctively different from 1st crisis. A much smaller telomere elongation, only to 3.7 kb, was measured with the occurrence of an additional high molecular weight band at ~16 kb. After the 2nd crisis, the length of the short telomeres stabilized whereas long telomeres continuously shortened, with both fractions merging toward the end of the experiment. Southern blot analysis for the dominant-negative hTERT verified that there was no cellular contamination and that the original insertion site persisted throughout the experiment (data not shown).

In situ hybridization with a telomere-specific probe after 2nd crisis confirmed the TRF result (Fig. 1*B*). We observed some short chromosomal ends lacking telomeric signal. In addition, we observed chromosomal end-to-end fusions as a consequence of the 1st crisis event as well as long telomeric ends that correspond to the high molecular weight band detected in the TRF analysis (Fig. 1*B*).

Telomerase Activity During Two Crisis Events in an MSH6 −/− Cell Clone. To analyze the nature of the two-telomere elongation events shown in Fig. 1*A*, we performed telomerase activity (TRAP) assays at each time point when TRF analysis was done. As illustrated in Fig. 2*A*, inhibition of telomerase activity by expression of a dominant-negative hTERT was robust (up to 127 PDs) with residual levels ranging from <0.5–1.1% compared with the parental cell line. Notably, the two crisis events were not associated with detectable up-regulation of telomerase activity but rather with the same levels as observed during the period of telomere shortening. However, after PD 127 up-regulation of telomerase, activity appeared with a constant increase in activity toward the

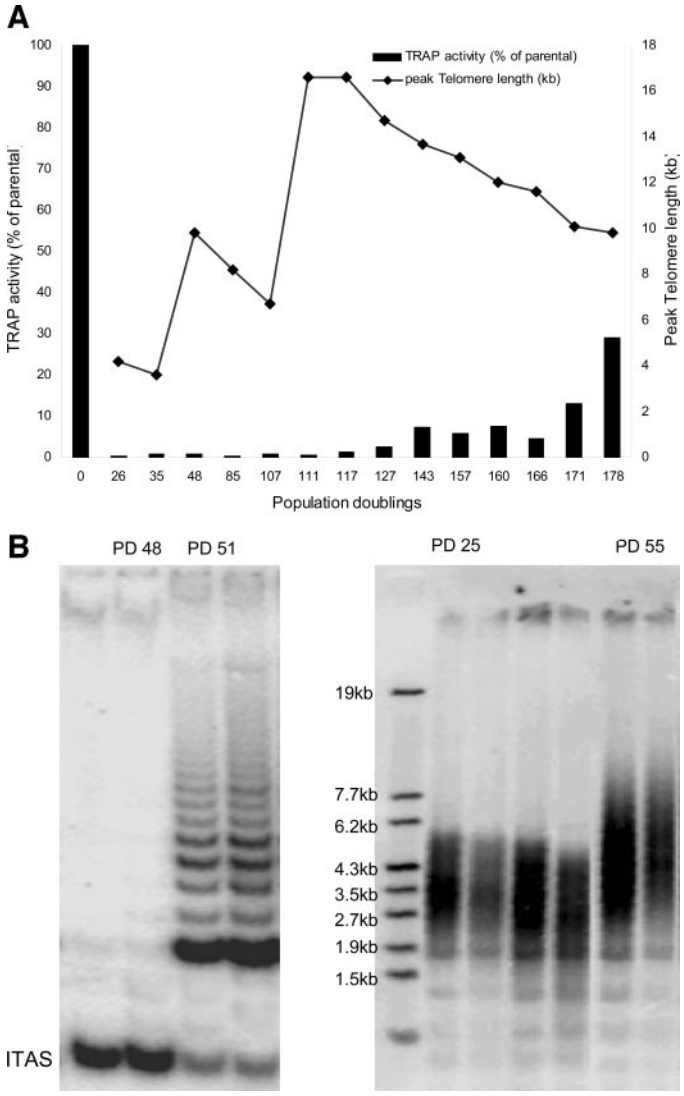

Fig. 2. *A*, telomerase activity during telomere length undulation. Inhibition of telomerase was initially robust, with levels lower than 1% of the levels of the parental cell line (point 0). The line graph shows the course of peak telomere length throughout the experiment. Notably neither 1st nor the 2nd crisis event was associated with detectable up-regulation of telomerase activity. After population doubling 127, telomerase activity slowly increases whereas the high molecular weight band gradually shortens. *B*, TRAP activity and telomere length in an HCT 15/dominant-negative human telomerase reverse transcriptase clone re-expressing telomerase activity after crisis. Cells emerging from crisis at population doubling 51 show a strong reappearance of telomerase activity, which leads to elongation and further stabilization of telomere length in cells after crisis. Four of five HCT 15/dominant-negative human telomerase reverse transcriptase clones showed this behavior. *TRAP*, telomere repeat amplification protocol.

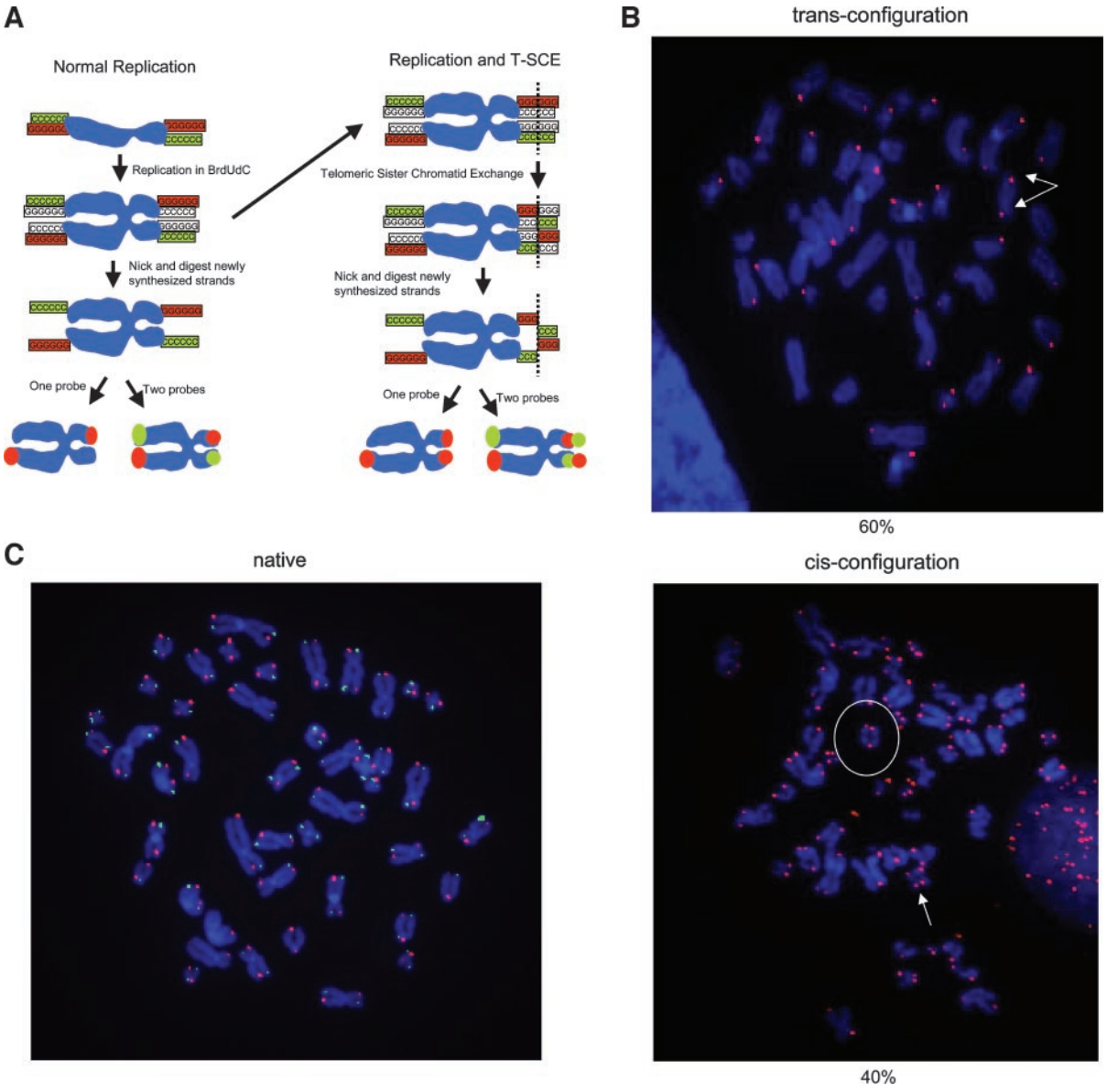

Fig. 3. *A*, CO-FISH analysis is able to detect telomeric sister chromatid exchange. DNA replication in the presence of bromodeoxyuridine and 5-bromodeoxycytidine allows degradation of the newly synthesized daughter strands. Hybridization with either the G-rich probe or the C-rich probe reveals a single chromatid signal at each end. In case of T-SCE, hybridization with a single strand specific probe will result in a signal on the same end of sister chromatids. If T-SCE occurs at only one end of the chromosome, three signals can be detected (triplet); if both ends are involved, four signals are detected (quadruplet). Dual staining with two probes show a *yellow* signal attributable to colocalization of the two probes (C-rich probe labeled Cy3, G-rich probe labeled FITC for this example). *B*, CO-FISH analysis for leading strand in HCT 15 cells with critically short telomeres. Inhibition of telomerase activity leads to telomere shortening. In precrisis cells, staining telomeres with a probe for leading strand shows no T-SCE in 60% of the metaphases (*arrows* pointing to one signal at each chromatid pair). However in 40% of the metaphases, T-SCE affects more than half of the chromosomes. In two of three of the chromosomes, only one chromosomal end shows T-SCE whereas in one of three of the chromosomes both ends exhibit a T-SCE signal. *C*, CO-FISH analysis in cells after crisis with up-regulation of telomerase activity. In a HCT 15 clone where cells escape from crisis because of up-regulation of telomerase activity, stabilization of telomeres occurs. T-SCE was completely abolished in all metaphases analyzed (dual staining shown for leading strand = *red* and lagging strand = *green*). *T-SCE*, telomeric sister chromatid exchange.

end of the experiment. To increase telomerase inhibition, we infected cells before as well as immediately after 2nd crisis with a second retrovirus encoding for a dominant-negative hTERT. In both cases the reappearance of telomerase activity could not be prevented, although Southern blot analysis did not show gene amplification as being the cause for telomerase reappearance (data not shown). Most other tested HCT 15 clones expressing a dominant-negative hTERT showed strong telomerase expression of cells emerging from crisis and did not show telomere length fluctuations as shown in Fig. 1*A* (Fig. 2*B*). Because of the reappearance of telomerase, telomeres were stabilized and maintained at a constant length beyond the point of crisis. In addition to following HCT 15 cell clones with inhibited telomerase activity ($n = 5$), we also analyzed colorectal cancer cell lines with other MMR defects. Neither clones of cells with hMSH2 −/− (Lovo, $n = 3$) or human mutL homolog 1 −/− (HCT 116, $n = 3$) nor cancer cells with a wild-type MMR phenotype (SW 480, $n = 2$) showed the same telomere length kinetics as shown for the HCT 15 cells. For all other clones, either cell death and loss of the culture or reappearance of telomerase activity occurred as a consequence of crisis.

Telomeric Recombination between Sister Chromatids (T-SCE) before and after Crisis. To investigate whether telomeric recombination was associated with this telomere elongation event, we applied a CO-FISH analysis to determine the presence of telomeric sister chromatid exchange within telomeres (Fig. 3*A*). After DNA replica-

tion in the presence of bromodeoxyuridine and 5-bromodeoxycytidine, newly synthesized leading and lagging daughter strands are present on different chromatids at each end of the chromosome. These strands can be removed by nicking the bromodeoxyuridine- and 5-bromodeoxycytidine-containing DNA by UV irradiation in the presence of Hoechst 33258 and Exonuclease III digestion, leaving the parental strands intact. Hybridization with a strand-specific probe [*e.g.*, a FITC-conjugated $(TTAGGG)_3$] will then only give a signal on one of the two-paired chromatids at each end. If a sister chromatid exchange event has occurred within the telomeric sequences (T-SCE) both DNA strands are partially composed of parental and newly synthesized DNA, so that both sister chromatids will anneal to a single strand-specific probe. Applying this technique, we found that in a variety of different human ALT cell lines, T-SCE was present in 100% of the metaphases analyzed whereas T-SCE was universally missing in human telomerase-positive cells (Table 1). Inhibition of the ALT pathway by introducing telomerase exogenously strongly reduces all ALT-typical features in VA13 cells as reported previously (23). In addition, we found that T-SCE in VA13 +hTR/hTERT was drastically reduced in frequency and affected only 1–2 chromosomal ends per cell (data not shown). Fibroblasts in patients with conditions associated with an increased rate of normal sister chromatid exchange (*e.g.*, Bloom or Werner-syndrome display only very small increased frequencies of T-SCE), suggesting that those factors affecting general SCE do not have a great effect on telomeric sequences (Table 1). Elongation of the shortest telomeres in ALT cells by telomerase, or the absence of critically short telomeres in telomerase-positive cells may suppress T-SCE by removing a *trans*-acting T-SCE signal. We then compared telomeric sister chromatid exchange in a telomerase-reverting HCT 15 control clone to the clone with ALT characteristics described in Figs. 1 and 2*A*.

Immediately before entering crisis, an HCT clone with dominant-negative hTERT that re-expressed telomerase showed a normal phenotype in 60% of the metaphases, with a single chromatid signal at each end (Fig. 3*B*). Some telomeric ends did not hybridize to the G-rich probe because of the critically short telomeres observed before crisis. However, 40% of the metaphases show T-SCE with more than half of the chromosomes per metaphase spread being affected (approximately two of three of the chromosomes show T-SCE on only one chromosomal arm; in one of three of the chromosomes both ends show T-SCE). After cells re-expressing telomerase emerged from crisis, telomere length was stabilized and telomeric sister chromatid exchange could no longer be observed, indicating that telomerase up-regulation abolished T-SCE in 100% of the cases (Fig. 3*C*).

A different picture was observed for the cell clone showing telomere elongation but lacking the reappearance of telomerase activity throughout two crisis events. Cells analyzed with CO-FISH immediately after the 1st crisis, when a telomere elongation event had already occurred, showed no T-SCE in 13% of the metaphases analyzed. However, 87% of metaphases exhibited T-SCE (with 40–60% of the chromosomes per metaphase being affected), indicating an ongoing telomeric recombination process even after the cells emerged from crisis (Fig. 4*A*, only leading strand hybridization shown). A similar picture was found for cells immediately after the 2nd crisis, which generated the distinct high molecular weight DNA band of approximately 16 kb. In these cells, telomeric recombination was present after crisis in 60% of the metaphases analyzed, also involving the chromosomal end with the long telomere (Fig. 4*B yellow* colocalization signal of leading and lagging strand). In addition to CO-FISH, staining for APBs was done at various population doublings throughout the course. APB bodies showing colocalization of promyelocytic leukemia and TRF2 were not found at either 1st or 2nd crisis (data not shown).

MSH6 Substitution via Retroviral Overexpression. To determine whether the MSH6 −/− defect was required for the activation of an ALT-like phenotype in these cells, we overexpressed MSH6 protein in the HCT 15 clone that showed telomere elongation without detectable up-regulation of telomerase. MSH6 was overexpressed by retroviral infection before cells went into 1st crisis at PD 28. Control infections were done with an empty vector. After selection, clones at a size of ~1000 cells went into 1st crisis. Notably twice as many colonies could be generated for the control infection with the empty vector than for the MSH6 infection. After the colonies emerged from 1st crisis, cells were harvested for TRF, TRAP, and Western analysis. Clones infected with the MSH6-overexpressing vector as well as control-infected cells went through 1st crisis, showing the same pattern of telomere elongation followed by telomere shortening as shown in Fig. 1*A*. In addition, no TRAP activity was detected. When assayed for protein expression, we found that neither the control-infected cells nor the MSH6-infected cells expressed detectable amounts of MSH6, suggesting that a negative selection against MSH6-overexpressing cells had taken place (Fig. 5).

Tumor Formation of Cells with and without T-SCE. It has been shown previously that the ALT pathway does not substitute for telomerase in the process of tumorigenesis in *vivo* (15). We therefore sought to address the question whether or not cells with T-SCE show the same impairment of tumor formation. Cells escaping from 2nd crisis when T-SCE was observed (PD 110, before telomerase became reactivated; see Fig. 2*A*) were injected into two mice (test group). Control groups included injections with the HCT 15 parental cell line (two mice) and injection with cells rescued from 2nd crisis via hTERT infection (adenoviral hTERT; one mouse). hTERT overexpression after adenoviral infection restored telomerase activity abolished the appearance of the high molecular weight band observed after 2nd crisis (see Fig. 1) and inhibited T-SCE (data not shown). Assessment of tumor volume was done after 2 weeks. For one mouse of the test group tumor extirpation was done following 4 weeks after no change of tumor size was observed between week 2 and 4. Tumor volume for

Table 1 *Frequency of telomeric sister chromatid exchange in various immortalized cell lines*

Chromatid orientation fluorescence *in situ* hybridization analysis showed that ALT[a] cells display T-SCE, which is in contrast to telomerase-positive cells where no T-SCE is observed. Inhibition of ALT by ectopical expression of telomerase reduces T-SCE. Genetic conditions associated with increased sister chromatid exchange do not show elevated T-SCE in the presence of telomerase activity.

Cell line	T-SCE+ metaphases/ metaphase analyzed		Characteristics
MDA 041	0/15	Telomerase	Li Fraumeni-syndrome fibroblasts (p53±)
MDA 087	20/20	ALT	Li Fraumeni-syndrome fibroblasts (p53 ±)T-SCE involves the majority of chromosomal ends
VA-13	13/13	ALT	T-Ag immortalizedT-SCE involves the majority of chromosome ends
VA-13+hTR/hTERT	6/20		T-SCE present in only 1–2 chromosome ends in some of the metaphases
SW 13	20/20	ALT	T-Ag immortalizedT-SCE involves the majority of chromosome ends
Hela	0/20	Telomerase	
Werner (hTERT)	1/20	Telomerase	T-SCE present in only 1–2 chromosome ends in one of the metaphases
Bloom (hTERT)	3/20	Telomerase	T-SCE present in only 1–2 chromosome ends in a few of the metaphases

[a] ALT, alternative lengthening of telomeres; hTERT, human telomerase reverse transcriptase; T-SCE, telomeric sister chromatid exchange.

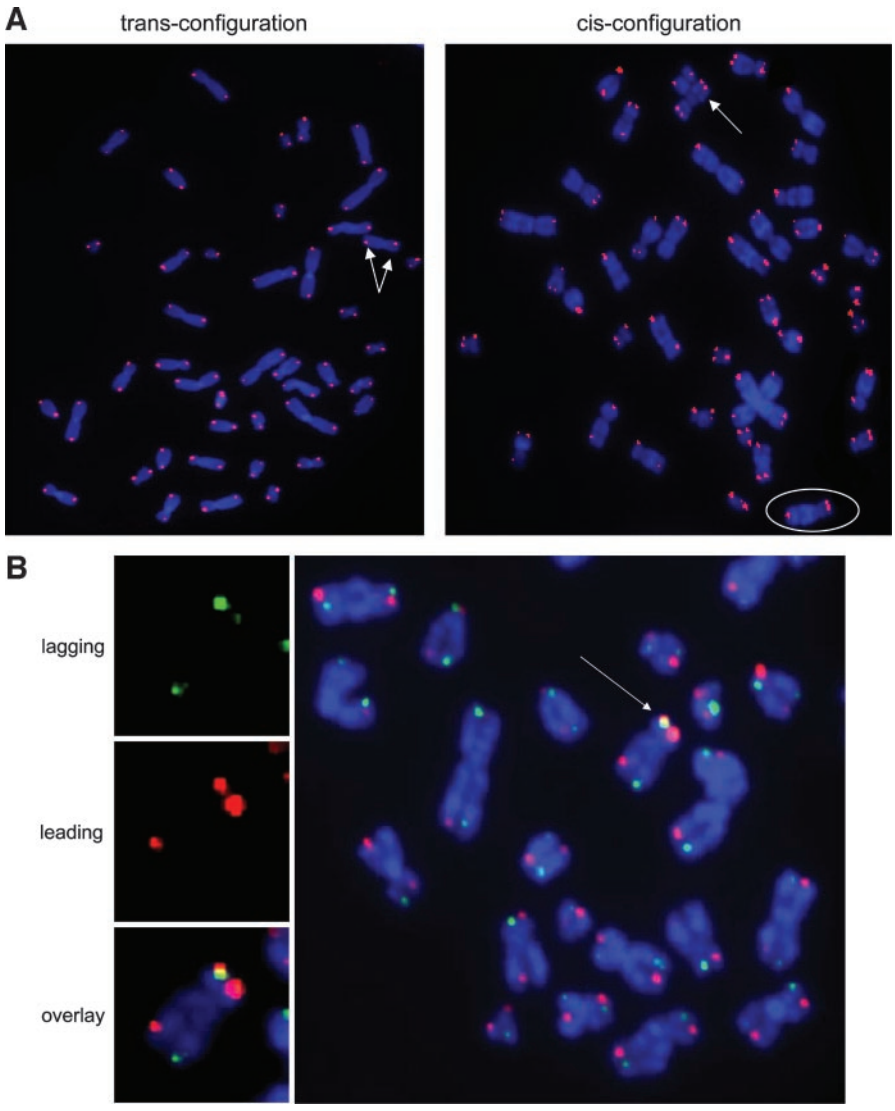

Fig. 4. *A*, CO-FISH analysis in cells escaping from 1st crisis without detectable telomerase up-regulation. In 13% of the metaphases, no telomeric sister chromatid exchange could be seen (shown for the leading strand). Persistent telomeric recombination however is present in many chromosomes in the majority of metaphases in cells after 1st crisis (triplets, *circle*; quadruplets, *arrow*; ratio, approximately two of three to one of three). *B*, CO-FISH analysis in cells escaping from 2nd crisis without detectable telomerase up-regulation. After 2nd crisis, telomeric recombination was present similar to after the 1st crisis, also involving the long telomeric end that appears as the ~16 kb high molecular weight band in telomere restriction fragment analysis. Leading strand and lagging strand sequences are present on the same chromosomal arm thereby appearing as a *yellow* signal.

the HCT 15 parental cell line was 297.5 mm^3 at average (range 125–600 mm^3). Cells injected showing T-SCE formed smaller tumors with an average volume of 24.1 mm^3 (range, 0–62.5 mm^3; one flank showed no tumor formation). For the mouse receiving 2nd crisis cells infected with adenoviral hTERT, tumor volume measured 147.5 mm^3 at average (range, 50–245 mm^3; Fig. 6).

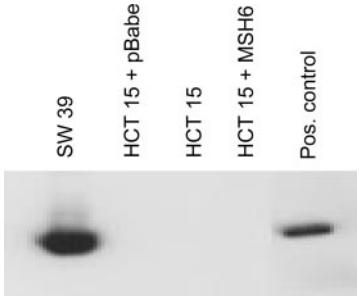

Fig. 5. Western analysis for MSH6 after retroviral overexpression. Cells were infected with MSH6 (pWZL-Blast MSH6) or an empty control vector (pBabe Puro) before 1st crisis and went through 1st crisis as a population. Western analysis performed after first crisis showed no expression of MSH6 in infected HCT 15 cells despite resistance to the selectable marker. Positive control: HCT 15 transient transfected with PWZL-Blast MSH6; 50 μg of protein/lane except for the positive control (10 μg); SW39: MSH6 +/+ fibroblast cell line.

DISCUSSION

The present results show that telomere elongation can occur without detectable up-regulation of telomerase activity when telomerase is inhibited in a MMR-defective background. Previous reports of inhibiting telomerase have either resulted in cell death or the reappearance of cells with telomerase activity (24, 25). In addition, we show that telomeric recombination within sister chromatids coincides with short telomeres in cells in crisis, suggesting that enhanced telomeric sister chromatid exchange is associated with an ongoing DNA damage signal in those cells. We further show that telomerase activity abolishes telomeric recombination, suggesting that elongating critically short telomeres removes a *trans*-acting signal that stimulates T-SCE. Importantly, telomeric recombination within sister chromatids is still present after this clone of MSH6 −/− cells escaped from crisis without detectable up-regulation of telomerase, suggesting that an ALT-like pattern of recombination had taken place. Tumor formation experiments in nude mice further showed that cells displaying T-SCE after emerging from crisis do not form robust tumors. This is in sharp contrast to the telomerase-positive parental cells or to cells with abolished T-SCE caused by exogenous telomerase overexpression.

Our knowledge of telomere length kinetics in the absence of telomerase activity and subsequent engagement of the ALT pathway

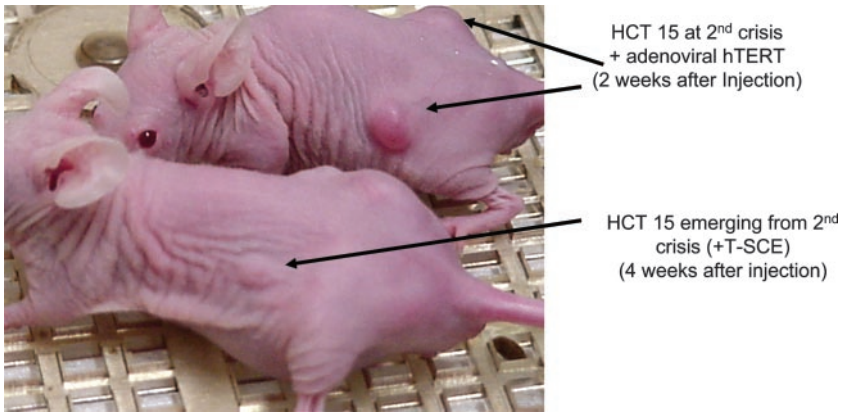

Fig. 6. Tumor formation in nude mice. Mice were injected with cells immediately after emerging from 2nd crisis (at population doubling 110, see also Fig. 2*A*) either without (T-SCE ongoing) or after being treated with adenoviral hTERT (T-SCE abolished). After 2 weeks, adeno-hTERT cells formed tumors (245 mm^3) whereas mice injected with cells in which T-SCE was ongoing showed only small tumors after 4 weeks of observation (2 mm^3). *hTERT*, human telomerase reverse transcriptase; T-SCE, telomeric sister chromatid exchange.

comes primarily from work in yeast. For yeast, two different phenotypes of telomerase-independent survivors have been described. Type I survivors are characterized by amplification of subtelomeric repeats (Y′ elements) flanking short stretches of G-rich telomeric repeats. In contrast, type II survivors show a broad range of telomere lengths more reminiscent of the ALT phenotype in human cells (26). The fact that both classes of survivors are dependent on radiation sensitive protein 52 (Rad 52) function stresses the role of homologous recombination in these survivors. Lundblad and Blackburn (27) proposed a model in which short telomeres produced by the absence of telomerase become more recombinogenic, and that recombination occurs in a burst that is triggered by critically short telomeres. This model is supported by several recent studies (14, 28). Short telomeres in *Sacchromyces cerevisiae* maintained by a partly active telomerase showed vastly up-regulated recombination rates of a marker gene placed in the subtelomeric region, resembling the amplification of Y′elements in type I survivors of yeast. Looking at type II survivors in yeast, Teng *et al.* (29) found that gradual telomere shortening in precrisis cells was followed by abrupt elongation events, which were associated by an improved growth rate of the culture. A similar observation with regard to telomere kinetics was made in an established human ALT cell line (30). Marked telomeres showed gradual shortening followed by a sudden elongation event.

We cannot rigorously rule out a short burst of telomerase reactivation when the cells reached crisis. However, barely detectable telomerase levels were identical before and after each crisis event, and no obvious telomerase up-regulation was seen despite careful analysis. It is therefore unlikely that telomerase is the cause for the observed telomere elongation. Overexpression of telomerase by adenoviral infection of cells during 2nd crisis resulted in a different type of telomere elongation. T-SCE as well as the distinct high molecular weight band formerly observed after 2nd crisis was no longer present, suggesting that telomerase activity inhibited recombination. In addition, the persistence of telomeric sister chromatid recombination even after cellular crisis compared with a telomerase-dependent control clone argues for a telomerase-independent recombination-based mechanism. This is even more emphasized by the observation that T-SCE is tightly associated with the presence of an ALT phenotype. The reason why we did not observe a complete engagement of the ALT pathway in its classical definition is most likely attributable to the eventual reappearance of telomerase. Once telomerase was present, telomeres stabilized and T-SCE vanished. The lack of APB bodies could be attributable to the same reason, because these structures have been described only in fully developed ALT cells.

The precise role of a MMR defect for the engagement of this ALT-like telomere elongation remains unclear. The concept that a hyper-recombinogenic phenotype, which is associated with the MMR defect, facilitates ALT engagement is supported by recent work in yeast (14). In this study Rizki and Lundblad observed that a double knock out for telomerase (est2-Δ) and msh2 (msh2-Δ) increases the survival of telomerase-deficient cells. They also observed an immediate growth advantage of the msh2-Δ and est2-Δ yeast strain over the est2-Δ strain alone, suggesting the result was not attributable to a secondary consequence of the mutator phenotype associated with the msh2-Δ defect. Although the data obtained from the yeast system argue against any causal role for the mutator phenotype, this cannot be unambiguously translated into the human system at this point. The infrequent appearance of the phenomenon described for other MMR-deficient cell clones suggests that MMR causes a secondary alteration that facilitates ALT-like telomeric recombination associated with the presence of T-SCE. This notion is even more strongly supported by the fact that MSH6 deficiency is associated with a strong mutator phenotype (18). If this would be the case, MSH6 substitution would not abolish the ALT-like behavior of the cells we describe in this present work. Unfortunately, overexpression of MSH6 was associated with cellular toxicity as reported previously, and therefore systems providing a more subtle transcriptional regulation of MSH6 will be needed (18).

It has been shown that ALT cells exhibit a much less tumorigenic potential compared with telomerase-positive cells (15). This lack of tumor formation was overcome by introducing the Ras oncogene together with hTERT, whereas Ras alone did not restore the tumor formation potential. In addition, recent work by Chang *et al.* (31) provides evidence that ALT-positive tumors derived from telomerase knockout mice are unable to form lung metastases in a mouse model. Reconstitution of telomerase in these ALT-positive tumors rendered these cells competent to form metastatic lesions. Together these data suggest that the ALT pathway, at least for some cell lines, does not functionally substitute for telomerase as far as tumorigenicity and metastatic potential is concerned. A likely explanation is the presence of telomere dysfunction in ALT cells caused by a number of critically short telomeres in these cells (23). The tight correlation between T-SCE and the ALT pathway, as shown in this present work, makes telomeric sister chromatid exchange a new cytogenetic ALT marker. The data also suggest that T-SCE might be a response to the DNA damage signal from dysfunctional short ends. Importantly, T-SCE can occur in non-ALT cells. T-SCE was observed before crisis in a clone of HCT cells with a dominant-negative hTERT that eventually escaped crisis by re-expressing telomerase activity. This demonstrates that T-SCE is not equivalent to ALT, is probably not directly involved in ALT-like telomeric elongation events, but rather reflects a process that is occurring at a very highly elevated rate in ALT cells that might contribute indirectly to telomere elongation. Its very strong correlation with ALT nonetheless makes it a useful marker for ALT cells. Our

results from tumor formation experiments demonstrate, similar to previous reports, that cancer cells emerging from crisis with T-SCE being present induce smaller tumors compared with the telomerase-positive parental cells. More importantly abolishing T-SCE via overexpression of telomerase restores the tumor formation capacity.

Our data show that an ALT-like telomere elongation is possible when telomerase is inhibited in conjunction with an MSH6 defect. Although these escaping cancer cells might not be as robust as their telomerase-positive counterparts, this observation has an impact on therapeutic concepts involving telomerase inhibitors. The possibility of telomere elongation without significant telomerase activity could make some human malignancies less suitable for telomerase-inhibitory therapeutics and hence could be a drug resistance mechanism. Importantly, future experiments using this model system for engaging ALT may provide insights and screening strategies for repressing this pathway.

ACKNOWLEDGMENTS

We thank V. Lundblad for helpful discussions. Susan M. Bailey and Edwin H. Goodwin have reported similar findings in murine cells (unpublished results).

REFERENCES

1. Watson JD. Origin of concatemeric T7 DNA. Nat New Biol 1972;239:197–201.
2. Olovnikov AM. Telomeres, telomerase, and aging: origin of the theory. Exp Gerontol 1996;31:443–8.
3. Jacob NK, Kirk KE, Price CM. Generation of telomeric G strand overhangs involves both G and C strand cleavage. Mol Cell 2003;11:1021–32.
4. Smogorzewska A, de Lange T. Different telomere damage signaling pathways in human and mouse cells. EMBO J 2002;21:4338–48.
5. Wright WE, Pereira-Smith OM, Shay JW. Reversible cellular senescence: implications for immortalization of normal human diploid fibroblasts. Mol Cell Biol 1989; 9:3088–92.
6. Greider CW, Blackburn EH. The telomere terminal transferase of Tetrahymena is a ribonucleoprotein enzyme with two kinds of primer specificity. Cell 1987;51:887–98.
7. Shay JW, Bacchetti S. A survey of telomerase activity in human cancer. Eur J Cancer 1997;33:787–91.
8. Henson JD, Neumann AA, Yeager TR, Reddel RR. Alternative lengthening of telomeres in mammalian cells. Oncogene 2002;21:598–610.
9. Dunham MA, Neumann AA, Fasching CL, Reddel RR. Telomere maintenance by recombination in human cells. Nat Genet 2000;26:447–50.
10. Bechter OE, Zou Y, Shay JW, Wright WE. Homologous recombination in human telomerase-positive and ALT cells occurs with the same frequency. EMBO Rep 2003;4:1138–43.
11. Shay JW, Wright WE. Telomerase: a target for cancer therapeutics. Cancer Cell 2002;2:257–65.
12. Rayssiguier C, Thaler DS, Radman M. The barrier to recombination between Escherichia coli and Salmonella typhimurium is disrupted in mismatch-repair mutants. Nature (Lond) 1989;342:396–401.
13. Elliott B, Jasin M. Repair of double-strand breaks by homologous recombination in mismatch repair-defective mammalian cells. Mol Cell Biol 2001;21:2671–82.
14. Rizki A, Lundblad V. Defects in mismatch repair promote telomerase-independent proliferation. Nature (Lond) 2001;411:713–6.
15. Stewart SA, Hahn WC, O'Connor BF, et al. Telomerase contributes to tumorigenesis by a telomere length-independent mechanism. Proc Natl Acad Sci USA 2002;99: 12606–11.
16. Ouellette MM, Aisner DL, Savre-Train I, Wright WE, Shay JW. Telomerase activity does not always imply telomere maintenance. Biochem Biophys Res Commun 1999;254:795–803.
17. Herbert BS, Wright AC, Passons CM, et al. Effects of chemopreventive and antitelomerase agents on the spontaneous immortalization of breast epithelial cells. J Natl Cancer Inst (Bethesda) 2001;93:39–45.
18. Lettieri T, Marra G, Aquilina G, et al. Effect of hMSH6 cDNA expression on the phenotype of mismatch repair-deficient colon cancer cell line HCT15. Carcinogenesis 1999;20:373–82.
19. Wright WE, Tesmer VM, Liao ML, Shay JW. Normal human telomeres are not late replicating. Exp Cell Res 1999;251:492–9.
20. Chai W, Ford LP, Lenertz L, Wright WE, Shay JW. Human Ku70/80 associates physically with telomerase through interaction with hTERT. J Biol Chem 2002;277: 47242–7.
21. Goodwin E, Meyne J. Strand-specific FISH reveals orientation of chromosome 18 alphoid DNA. Cytogenet Cell Genet 1993;63:126–7.
22. Bailey SM, Goodwin EH, Meyne J, Cornforth MN. CO-FISH reveals inversions associated with isochromosome formation. Mutagenesis 1996;11:139–44.
23. Ford LP, Zou Y, Pongracz K, Gryaznov SM, Shay JW, Wright WE. Telomerase can inhibit the recombination-based pathway of telomere maintenance in human cells. J Biol Chem 2001;276:32198–203.
24. Herbert B, Pitts AE, Baker SI, et al. Inhibition of human telomerase in immortal human cells leads to progressive telomere shortening and cell death. Proc Natl Acad Sci USA 1999;96:14276–81.
25. Delhommeau F, Thierry A, Feneux D, et al. Telomere dysfunction and telomerase reactivation in human leukemia cell lines after telomerase inhibition by the expression of a dominant-negative hTERT mutant. Oncogene 2002;21:8262–71.
26. Teng SC, Zakian VA. Telomere-telomere recombination is an efficient bypass pathway for telomere maintenance in Saccharomyces cerevisiae. Mol Cell Biol 1999;19: 8083–93.
27. Lundblad V, Blackburn EH. An alternative pathway for yeast telomere maintenance rescues est1- senescence. Cell 1993;73:347–60.
28. McEachern MJ, Iyer S. Short telomeres in yeast are highly recombinogenic. Mol Cell 2001;7:695–704.
29. Teng SC, Chang J, McCowan B, Zakian VA. Telomerase-independent lengthening of yeast telomeres occurs by an abrupt Rad50p-dependent, Rif-inhibited recombinational process. Mol Cell 2000;6:947–52.
30. Murnane JP, Sabatier L, Marder BA, Morgan WF. Telomere dynamics in an immortal human cell line. EMBO J 1994;13:4953–62.
31. Chang S, Khoo CM, Naylor ML, Maser RS, DePinho RA. Telomere-based crisis: functional differences between telomerase activation and ALT in tumor progression. Genes Dev 2003;17:88–100.